IEEE Access
Multidisciplinary | Rapid Review | Open Access Journal

Received September 12, 2019, accepted October 4, 2019, date of publication October 9, 2019, date of current version October 22, 2019.

Digital Object Identifier 10.1109/ACCESS.2019.2946351

Sensitivity Analysis About Transient Three-Dimensional IHCP With Multi-Parameters in an Elbow Pipe With Thermal Stratification

WENWEN HAN[1,2], TAO LU[3], AND HONGBO CHEN[1]

[1]College of Electromechanical Engineering, Qingdao University of Science and Technology, Qingdao 266061, China
[2]National Engineering Laboratory for Advanced Tire Equipment and Key Materials, Qingdao University of Science and Technology, Qingdao 266061, China
[3]College of Mechanical and Electrical Engineering, Beijing University of Chemical Technology, Beijing 100029, China

Corresponding author: Hongbo Chen (qustchenhongbo@vip.163.com)

This work was supported by the National Natural Science Foundation of China (No. 51276009) and the Natural Science Foundation of Shandong Province (No. ZR2019BEE056).

ABSTRACT Pipelines with thermal stratification are common in nuclear power plants, and the thermal stratification may induce thermal fatigue and lead to leakage, so thermal stratification analysis of the pipeline is particularly significant. Due to the requirement of structural integrity, for the piping system of nuclear power plants, it is not allowed to trepan for installing sensors to measure the internal parameters. The inverse heat conduction problem (IHCP) based on the easily available temperature information of the outer wall can precisely estimate the boundary conditions of the inner wall. However, the precision of inverse estimation is influenced by the measuring precision, the number and the arrangement of measuring points. This work aims at the sensitive analysis about the measuring errors and the number and locations of measuring points. The research is based on an elbow pipe with thermal stratification—a pipe type commonly used in industry. Because it is easy to disturb the flow field to install sensors inside the pipeline, and it is difficult to calculate the convective heat transfer coefficient, the numerical experiments are taken in this study. The results showed that the IHCP with multi-parameters had certain anti-noise property and the number and locations of the measuring points had a certain influence on the calculation accuracy.

INDEX TERMS Convective heat transfer coefficient, elbow pipe, inverse heat conduction problem, sensitivity analysis, transient temperature distribution.

I. INTRODUCTION

Metal pipes are widely used in industry. However, material fatigue failure caused by thermal stress is common [1]–[3]. Therefore pipelines are also the most vulnerable to failure. Faulty pipelines can cause leak that can cause huge damages, especially in nuclear power plants. As early as 1988, the NRC issued statements, that all nuclear power plants, regardless in service or proposed, were required to complete thermal stratification analysis and risk assessment of surge lines to ensure structural integrity [4], [5]. It can be seen the importance of thermal fatigue analysis for the pipe with thermal stratification.

The associate editor coordinating the review of this manuscript and approving it for publication was Hongwei Du.

Because of the importance of thermal stratification in nuclear power pipelines, many scholars have studied the thermal stratification of nuclear power pipelines. Most scholars have done numerical simulation research on thermal stratification of pipelines [6], [8]–[11]. Through this method, the thermal stratification phenomenon can be predicted and analyzed theoretically, however, this method is not suitable for long time prediction under variable working conditions. Some experimental research have been carried out on this phenomenon [12]–[14], but only some specific working conditions of some specific models could be studied and summarized, without universality and strong adaptability. Some scholars [15] carried out fatigue monitoring on the surge lines through fixing thermocouples on the top and bottom of the outer wall, in order to monitoring the thermal fatigue accumulation at the junction of the fluctuation tube caused

by thermal stratification effect. When analyzing the thermal fatigue accumulation caused by thermal stratification inside the pipe, the actual internal temperature information of the surge pipeline cannot be allowed to measure directly by the thermocouple. In this work, the inverse heat conduction problem (IHCP) has been employed to estimate the convective heat coefficient and temperature data inside the elbow pipe made of stainless steel. The IHCP uses temperature information which can be obtained easily to estimate parameters whose values can only be obtained with difficulty. In previous work, the method has been employed to solve for variables such as boundary conditions [7], [16]–[24], boundary shapes [25]–[27], thermophysical properties of a physical model [28]–[30] and source terms [29], [31]–[33].

The IHCP consists of a direct problem and an inverse problem. The inverse problem uses a specific optimization method to update the estimated variables, and then the updated variables are assigned to the direct problem to solve the problem of fixing the solution. Methods for solving the IHCP include the conjugate gradient method (CGM) [34], the maximum entropy method (MEM) [35], the regularization solution [36], the neural network method (NNM) [37]–[40] and so on. These methods can be classified into stochastic and gradient-based ones. Although it is easy to search for the global optimum using stochastic methods, the methods have poor convergence and usually require a large computational effort. In contrast, gradient-based methods have fast convergence speed and high accuracy [41]. Therefore, in this work a gradient-based method—CGM—is chosen to solve the IHCP. There are various methods available to solve the direct problem, such as the finite difference method (FDM), the finite element method (FEM), the finite volume method (FVM), and the boundary element method (BEM) [42]. In this work, the FEM is chosen because of its convenience for solving the sensitivity matrix.

IHCP is widely used in all walks of life, such as nondestructive inspection [43]–[45], aerospace [46], food preservation [47], nuclear power [17]–[20] and so on. The application in nuclear power is mainly about the inverse estimation of some unmeasured parameters in pipelines with thermal stratification. In previous studies, some only inverse estimate the temperature of the near-wall fluid of the pipe [17], and some only inverse estimate the temperature of the inner wall of the pipe [18]. In order to obtain the boundary conditions of convective heat transfer on the inner wall of the pipeline, a model for solving the transient IHCP with multi-parameters was constructed in our previous research and verified by experiments [19], [20]. However, there are often errors in the actual measurements, and the influence of errors on inverse estimated results cannot be ignored. The number and location of measuring points on the outer wall in the actual projects are not only related to the project cost, but also have certain influence on the accuracy of inverse estimation. Therefore, the sensitivity analysis of the transient IHCP with multi-parameters is carried out in this work. The sensitivity analysis mainly refers to the research about the influence of measurement errors and the number and position of measuring points on the inverse estimation accuracy of heat transfer boundary conditions of the inner wall.

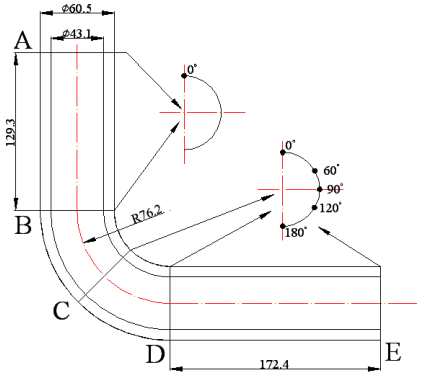

FIGURE 1. Physical model and locations of the measuring points.

An elbow pipe with thermal stratification is studied in this work. The convective heat transfer coefficient and the temperature of the fluid near the inner wall are the estimated parameters, and the temperature data of the outer wall that can be measured in actual engineering is the known conditions for solving the IHCP. Because the convective heat transfer coefficient is significantly influenced by the flow state, a measurement of the temperature of the fluid could disturb the flow field, so the temperature of the fluid near the inner wall and the convective heat transfer coefficient are estimated simultaneously. These form an IHCP with multi-parameters. The full solution to the problem is rather difficult and time-consuming. However, since there is almost no change in the flow conditions over time, we make the reasonable assumption that the convective heat transfer coefficient maintains an average value. Because it is easy to disturb the flow field to install sensors inside the pipeline, and it is difficult to calculate the convective heat transfer coefficient, the numerical experiments are taken in this study. Additionally, numerical experiments are more conducive to sensitivity analysis.

II. NUMERICAL EXPERIMENTS

As shown in Fig. 1, the elbow pipe was made of stainless steel with an outer diameter of 60.5 mm and an inner diameter of 43.1 mm. The vertical straight length was 129.3 mm, the horizontal straight length was 172.4 mm and the bend radius was 76.2 mm. The heat conductivity coefficient was $\lambda = 19.35\mathrm{W}/(\mathrm{m} \cdot K)$. In the direct problem, the inner wall was subject to the convective boundary condition, where the heat convection coefficient was $2000\mathrm{W}/(\mathrm{m}^2 \cdot \mathrm{K})$. The fluid in the pipe was water, and the fluid temperature near the inner wall was also measured. The outer wall was adiabatic The time step was $\Delta\tau = 1\ s$, and the total time was 80 s. Due to the symmetry in the physical model and the boundary conditions, only half of the elbow pipe was analyzed. In the direct heat conductin problem (DHCP), the hexahedral mesh was selected for this model, and the mesh number of

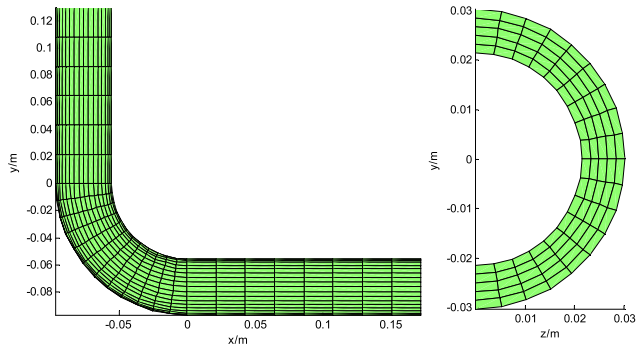

FIGURE 2. Meshes of Physical model.

this model was 2340 after grid independence verification. As shown in Fig. 2, the axial, circumaxial and radial mesh quantities were 26, 18 and 5, respectively.

The temperature fluctuations in the fluid near the inner wall at the measuring points on the cross sections A–E near the inner wall were obtained by experiment as shown in Fig. 3. In order to obtain the temperature distribution over time in the fluid near the inner wall, an interpolation was carried out for the whole fluid surface near the inner wall. As shown in Fig. 4(a), the fluid surface was divided into seven regions and different interpolation methods were employed in different regions.

The interpolations in regions F and G1 are shown in Fig. 4(a). The temperatures are determined by the linear interpolation in the vertical direction using the data at points cross section A-0°, cross section B-0° and cross section C-0°.

The research object in this work is an albow pipe with thermal stratification which is common in pressurizer surge line. Some previous researches reveale that the The thermal stratification phenomenon in elbow pipe mainly occurs at the corner of the pipe where the fluid temperature is distributed in layers along the vertical direction, and the temperature is basically the same in the horizontal direction of each layer [44], [45]. According to the above conclusions, it can be known that the temperature differences in the horizontal direction for regions G2, H1 and H3 are very small, so we assume that the temperatures on horizontal lines with the same y-coordinate are the same. For example, the temperatures at points P1 and P2 are equal to the temperature at point P, as shown in Fig. 4(b).

A linear interpolation was performed in regions H2 and I. For example, as shown in Fig. 4(b) the line N1N2 is horizontal and point M is located on the line N1N2. Although the temperature at point M is unknown, the temperatures at points N1 and N2 are known. Therefore a linear interpolation method can be performed to obtain the temperature at point M using Eq. (1).

$$T(M)=T(N1)\frac{X(N2)-X(M)}{X(N2)-X(N1)}+T(N2)\frac{X(M)-X(N1)}{X(N2)-X(N1)} \tag{1}$$

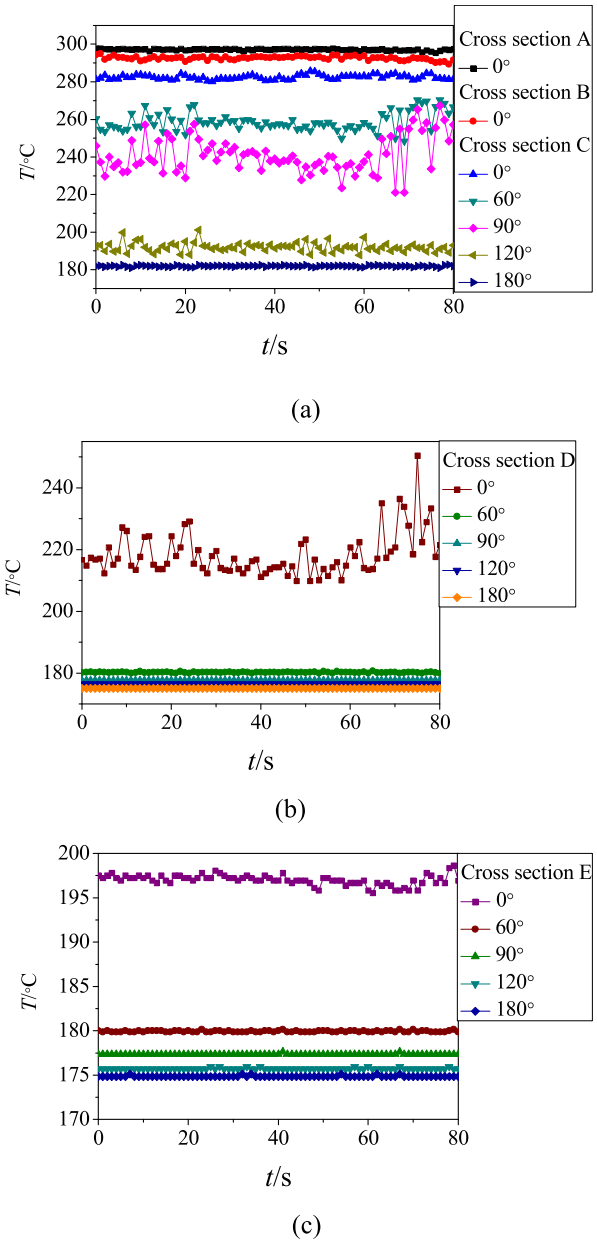

FIGURE 3. Fluid temperature fluctuations over time at the measuring points.

By means of interpolation, temperature information of all near-wall fluids at any moment has been obtained. Cross section D is located at the junction of elbow section and horizontal section, with obvious thermal stratification. As shown in Fig. 5, the fluid temperatures at 19 points (all nodes on this cross section in the physical model) on cross section D were obtained after a time of 50 s inside the elbow pipe. At each time step, the temperatures on both sides of the pipe for each cross section were assumed to be symmetric.

The temperature distribution of near-wall fluid at any moment can be obtained from the temperature values of all fluid nodes. For example, the temperature distribution of near-wall fluid at 50 s is shown in Fig. 6. It can be seen from

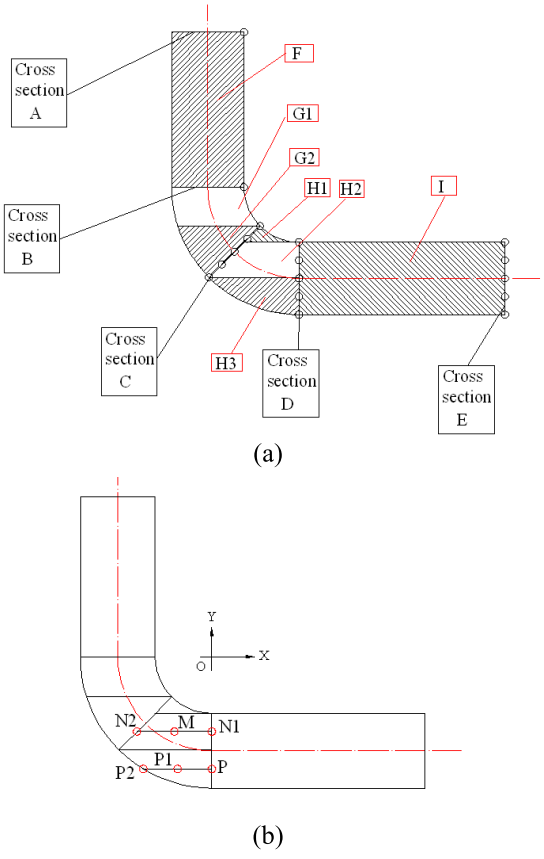

FIGURE 4. Interpolation of fluid temperature: (a) schematic diagram of fluid region division, (b) the diagram of linear interpolation.

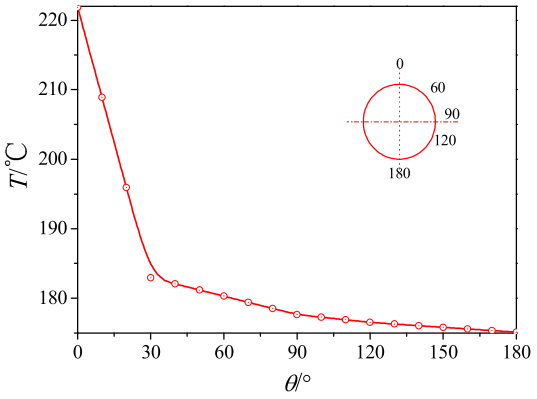

FIGURE 5. Linear interpolation results for cross section D at 50 s.

the figure that there is obvious thermal stratification of the near-wall fluid.

The governing equations, corresponding boundary conditions and initial condition for the transient direct heat conduction problem (DHCP) of the elbow pipe are:

$$\frac{\partial T}{\partial t} = \alpha\left(\frac{\partial^2 T}{\partial x^2} + \frac{\partial^2 T}{\partial y^2} + \frac{\partial^2 T}{\partial z^2}\right) \quad (x, y, z) \in \Omega \quad (2)$$

$$-\lambda\left(\frac{\partial T}{\partial n}\right)_{w,in} = h_{in}\left(T_{f,in} - T_{w,in}\right) \quad (x, y, z) \in \text{inner wall} \quad (3)$$

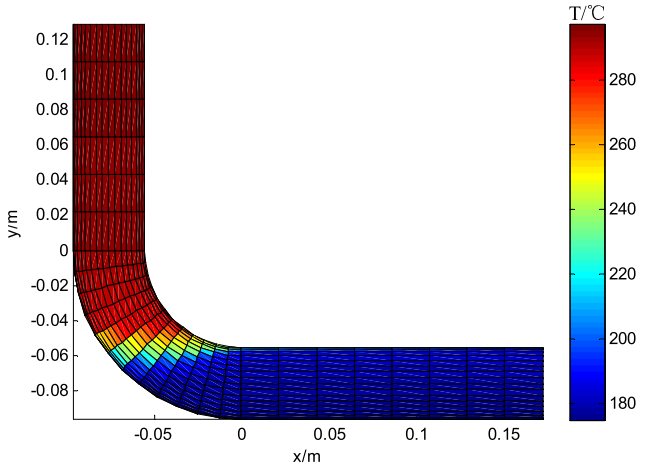

FIGURE 6. Fluid temperature distribution at 50 s.

$$-\lambda\left(\frac{\partial T}{\partial n}\right)_{w,out} = 0 \quad (x, y, z) \in \text{outer wall} \quad (4)$$

$$T(x, y, z, t) = T_0(x, y, z) \quad (x, y, z) \in \Omega, \ t = 0 \quad (5)$$

where T is the temperature of the nodes in the domain; α is the thermal diffusivity of the pipe, which has the value; x, y, z and t are the space and time variables; λ is the thermal conductivity of the pipe; n is the direction vector normal to the boundary wall;h_{in} is the convective heat transfer coefficient on the inner wall; T_w is the wall temperature and $T_{f,in}$ is the fluid temperature near the inner wall; the outer wall is adiabatic;$T_0(x, y, z)$ is the initial value of the pipe temperature.

The transient three-dimensional DHCP is solved using the Finite Element Method (FEM) based on the above known conditions. The temperatures of the whole solid domain including the inner wall and outer wall are all obtained after calculation. The temperature fluctuations over time at the measuring points cross section C-60°, cross section C-90°, cross section C-120° and cross section D-0° are shown in Fig. 7.

III. THE INVERSE HEAT CONDUCTION PROBLEM (IHCP)

In the IHCP, the temperature data of the outer wall are the input conditions for estimating the temperature data of the fluid and the convective heat coefficient near the inner wall. The IHCP can be mathematically considered as an optimization problem, i.e. the inversion parameters are optimized unceasingly at a certain optimization method, the DHCP will be solved based on the optimized inversion parameters and the temperature information of the outer wall will be obtained, and the function composed of the temperature information of the outer wall obtained from the numerical experiment and IHCP as the objective function. When the objective function reaches the minimum, it is considered that the estimated parameters of the IHCP are closest to the measured parameters of the numerical experiment, so as to obtain the optimal solution of the IHCP.

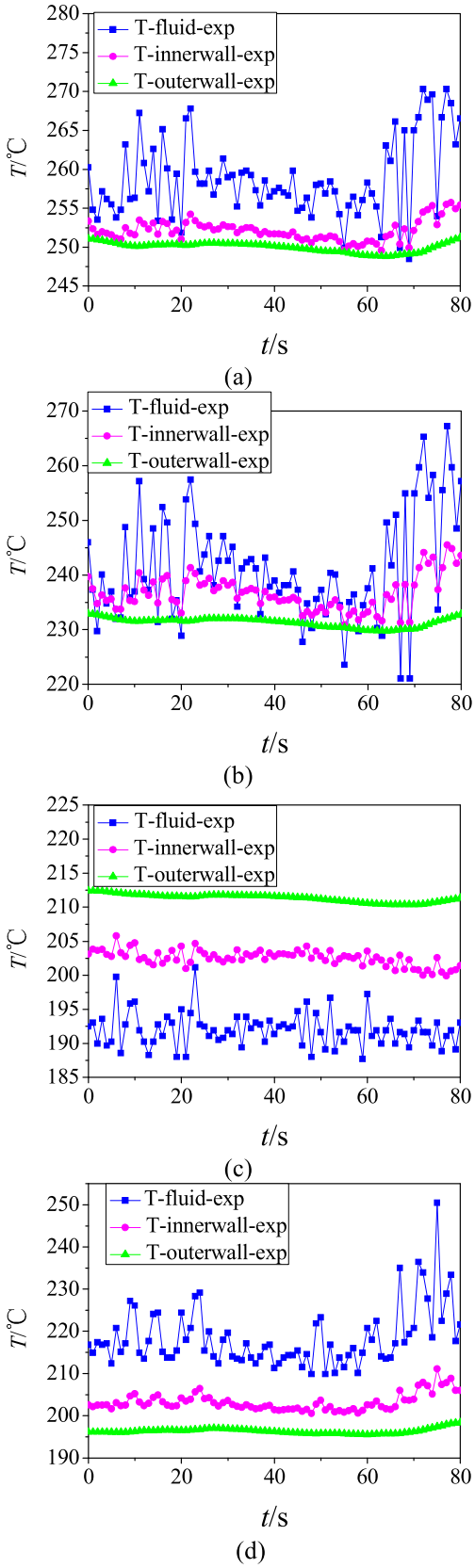

FIGURE 7. Temperature fluctuations over time at the measuring points: (a) cross section C-60°, (b) cross section C-90°, (c) cross section C-120° and (d) cross section D-0°.

The objective function is defined as

$$J(R) = \sum_{i=1}^{U}\sum_{j=1}^{V}\left[T_{i,j,est}(R) - T_{i,j,exp}\right] \tag{6}$$

where R is the parameter vector to be estimated, $R = \{r_1, r_2, \ldots, r_{nn+1}\} = \{T_{f,1}, T_{f,2}, \ldots, T_{f,nn}, h\}$. $T_{i,j,est}$ is the temperature data of outer wall obtained from IHCP; $T_{i,j,exp}$ is the temperature data of outer wall obtained from the numerical experiment; U is the number of time steps; V is the number of measuring points on the outer wall; nn is the number of fluid nodes.

Iteration termination condition of IHCP is

$$\left|J(R^b) - J(R^{b+1})\right| \le \mu \tag{7}$$

where b is the iterative steps; : μ is a small positive number, 0.001 is taken in this work.

Based on the Conjugate Gradient Method (CGM), the iterative formula of the inversion parameter vector R is

$$R^{b+1} = R^b - \beta^b d^b \tag{8}$$

where β^b is the iteration step length; d^b is the conjugate search direction, obtained by

$$d^b = \nabla J(R^b) + r^b d^{b-1} \tag{9}$$

where r^b is the conjugate coefficient, which can be obtained from the following equation

$$r^b = \frac{\nabla J(R^b)\nabla J^T(R^b)}{\nabla J(R^{b-1})\nabla J^T(R^{b-1})} \tag{10}$$

where $\nabla J(R^b)$ is the gradient of the objective function, i.e. $\nabla J(R^b) = (\partial J/\partial r_1, \partial J/\partial r_2, \cdots, \partial J/\partial r_{nn+1})$.

$$\frac{\partial J(R^b)}{\partial r_l} = 2\sum_{i=1}^{U}\sum_{j=1}^{V}\left[T_{i,j,est}(R) - T_{i,j,exp}\right]\frac{\partial T_{i,j,est}}{\partial r_i}, \quad l = 1, 2, \ldots, nn+1 \tag{11}$$

The iteration step length β^b can be obtained by optimizing the objective function:

$$\beta^b = \frac{\sum_{i=1}^{V}[T_i^{\mathrm{est}}(R^b) - T_i^{\mathrm{exp}}]\nabla T_i d^b}{\sum_{i=1}^{M}[\nabla T_i d^b]^2} \tag{12}$$

where ∇T_i is the sensitivity matrix and is a row vector:

$$\nabla T_i = \left(\partial T_i^{\mathrm{est}}/\partial r_1, \partial T_i^{\mathrm{est}}/\partial r_2, \cdots, \partial T_i^{\mathrm{est}}/\partial r_{nn+1}\right) \tag{13}$$

In this work, ∇T_i is determined by FEM. The specific methods are as follows:

A. THE SENSITIVITY ANALYSIS OF THE ITH NODE OF THE FLUID NEAR THE INNER WALL AT THE L TIME STEP

Partial derivatives of the governing equation, boundary conditions and initial conditions (equations (2)∼ (5)) of the DHCP with respect to T_f are calculated respectively, i.e

$$\frac{\partial}{\partial t}(\frac{\partial T}{\partial T_{f,i,l}}) = \alpha[\frac{\partial^2}{\partial x^2}(\frac{\partial T}{\partial T_{f,i,l}}) + \frac{\partial^2}{\partial y^2}(\frac{\partial T}{\partial T_{f,i,l}}) + \frac{\partial^2}{\partial z^2}(\frac{\partial T}{\partial T_{f,i,l}})] \quad (x,y,z) \in \Omega \tag{14}$$

$$-\lambda\frac{\partial}{\partial n}(\frac{\partial T}{\partial T_{f,i,l}})_{w,in} = h_{in}\left(\frac{\partial T_{w,in}}{\partial T_{f,i,l}} - \psi(i',l')\right) \quad (x,y,z) \in \text{inner wall}$$

$$\begin{cases} if\ i' = i, & l' = l\psi(i,l) = 1 \\ otherwise, & \psi(i,l) = 0 \end{cases} \tag{15}$$

$$-\lambda\frac{\partial}{\partial n}(\frac{\partial T}{\partial T_{f,i,l}})\Big|_{w,out} = 0 \quad (x,y,z) \in \text{outer wall} \tag{16}$$

$$\frac{\partial T}{\partial T_{f,i,l}} = 0 \quad (x,y,z) \in \Omega,\ t = 0 \tag{17}$$

By substituting equations (14) ∼ (17) into the finite element equation, the sensitivity matrix of T_f can be obtained.

B. THE SENSITIVITY ANALYSIS OF THE AVERAGE CONVECTIVE HEAT TRANSFER COEFFICIENT

Similarly, partial derivatives of the governing equation, boundary conditions and initial conditions (equations (2)∼ (5)) of the DHCP with respect to h_{in} are calculated respectively, i.e

$$\frac{\partial}{\partial t}(\frac{\partial T}{\partial h_{in}}) = \alpha[\frac{\partial^2}{\partial x^2}(\frac{\partial T}{\partial h_{in}}) + \frac{\partial^2}{\partial y^2}(\frac{\partial T}{\partial h_{in}}) + \frac{\partial^2}{\partial z^2}(\frac{\partial T}{\partial h_{in}})] \quad (x,y,z) \in \Omega \tag{18}$$

$$-\lambda\frac{\partial}{\partial n}(\frac{\partial T}{\partial h_{in}})_{w,in} = (T_{w,in} - T_{f,in}) + h_{in}\left(\frac{\partial T_{w,in}}{\partial h_{in}} - 0\right) = h_{in}\left(\frac{\partial T_{w,in}}{\partial h_{in}} - \frac{T_{w,in} - T_{f,in}}{h_{in}}\right) \quad (x,y,z) \in \text{inner wall} \tag{19}$$

$$-\lambda\frac{\partial}{\partial n}(\frac{\partial T}{\partial h_{in}})\Big|_{w,out} = 0 \quad (x,y,z) \in \text{outer wall} \tag{20}$$

$$\frac{\partial T}{\partial h_{in}} = 0 \quad (x,y,z) \in \Omega,\quad t = 0 \tag{21}$$

By substituting equations (18) ∼ (21) into the finite element equation, the sensitivity matrix of h_{in} can be obtained.

C. SOLUTION PROCEDURES AND PROCESSES OF THE TRANSIENT IHCP WITH MULTI-VARIABLES

The specific solving process of the three-dimensional IHCP with multi-parpmeters is as follows:

Step 1. Set the initial estimated parameters T_{f0} and h_{in0}, and the number of interation $b = 0$.

Step 2. Solve the DHCP Based on FEM and the estimated parameters, and obtained the estimated temperature data of the outer wall.

Step 3. Calculate the objective function $J_0(R)$ based on Eq. (6).

Step 4. Calculate the sensitivity matrix based on Eqs. (14) ∼ (21).

Step 5. Calculate the iteration step length β^b and conjugate search direction d^b based on Eqs. (9) ∼ (13), and update the estimated parameters based on Eq. (8).

Step 6. Repeat Step 3 and Step 4, obtain $J_1(R)$ based Eq. (6).

Step 7. Determine if the conditions are met Eq. (7). If so, stop the iteration; otherwise, set $J_1(R) = J_0(R)$ and go to step 4 to continue the calculation.

IV. RESULTS AND DISCUSSION

A. NOISE RESISTANCE ANALYSIS OF IHCP

In the analysis, there are no real experimental temperature data available for the inner wall and outer wall. Instead, the experimental temperature data for the fluid near the inner wall and the assumed convective heat transfer coefficient are employed in the DHCP to calculate the temperature data for entire temperature field of the pipe, including the temperature data of the outer wall and the inner wall. The results are taken as the computed temperature T_{DHCP}. However, in fact, there is always some degree of error in the temperature measurements. In order to consider these measurement errors, a random error noise is added to the above computed temperature T_{DHCP} to obtain the assumptive measured temperature T_{exp}. Hence, the measured temperature T_{exp} is expressed as:

$$T_{exp} = T_{DHCP} + \omega \cdot \sigma \tag{22}$$

where ω is a random variable within the range –1 to 1, and σ is the standard deviation of the measurement.

Four numerical cases with different values of σ (σ = 0.0, 0.1, 0.5, and 1.0) have been considered in this study in order to evaluate the accuracy and noise immunity of the CGM when predicting the convective heat transfer coefficient and fluid temperature. In the IHCP, the temperature of the outer wall, the boundary conditions at the outer wall and the physical properties of the elbow pipe are known. The assumptive experimental convective heat transfer coefficient is 2000 $W/(m^2 \cdot K)$, and the experimental temperature data for the fluid are shown in Fig. 3 and Fig. 6.

In order to examine the accuracy of the estimated data, the average relative error $\bar{\varepsilon}_h$ and $\bar{\varepsilon}_T$ for the convective heat transfer coefficient and the near-wall fluid temperature, and average absolute error $\bar{e}_T$ for the temperature of fluid near the inner wall are defined:

$$\bar{\varepsilon}_h = \frac{|h_{exp} - h_{est}|}{h_{exp}} \tag{23}$$

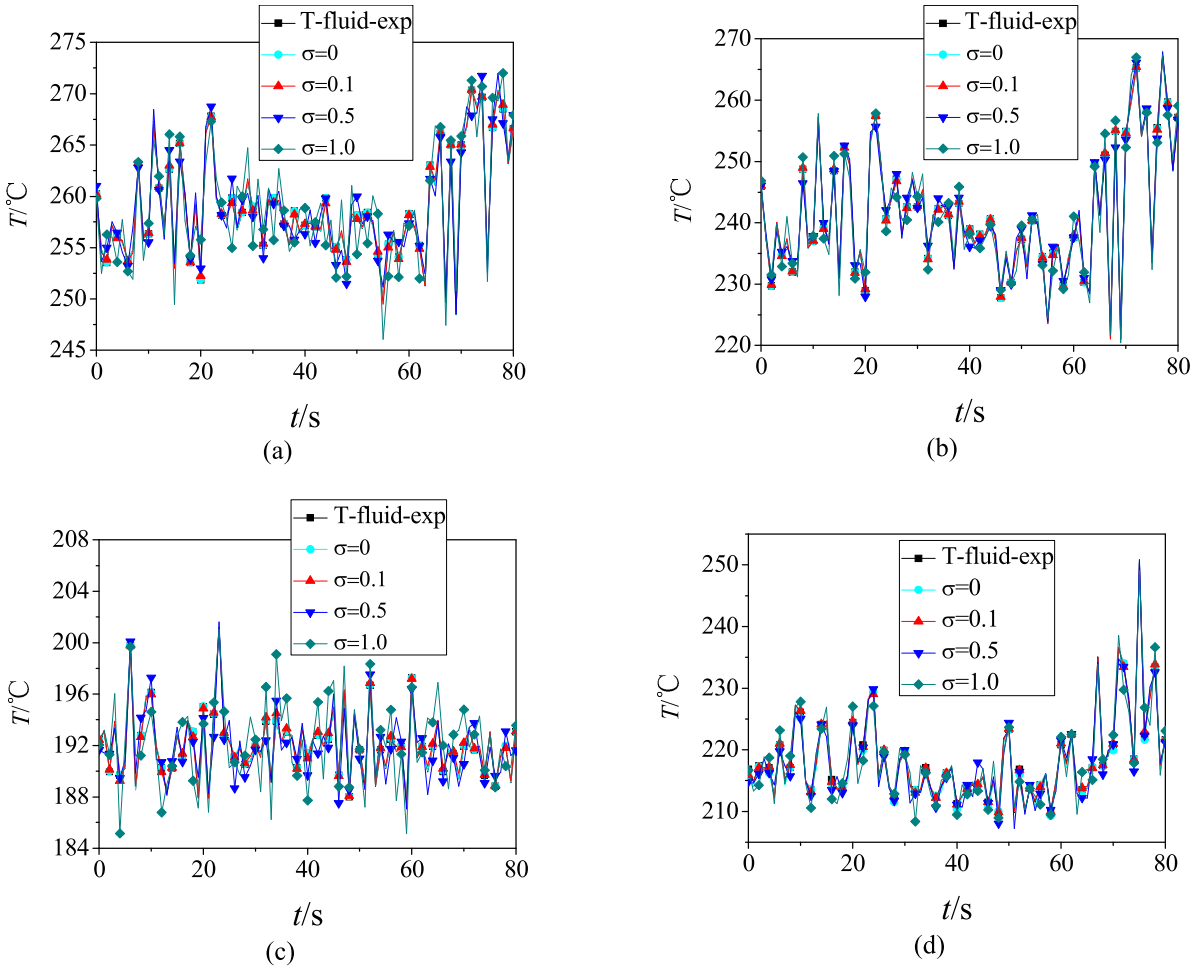

FIGURE 8. Experimental and estimated temperature data for the fluid near the inner wall at the measuring points: (a) C-60°, (b) C-90°, (c) C-120° and (d) D-0°.

$$\bar{\varepsilon}_T = \frac{1}{U}\sum_{t=1}^{U}\frac{\left|T_{exp}(t) - T_{cal}(t)\right|}{T_{exp}(t)} \tag{24}$$

$$\bar{e}_T = \frac{1}{U}\sum_{t=1}^{U}\left|T_{exp}(t) - T_{est}(t)\right| \tag{25}$$

where h_{exp} and h_{est} are the experimental and estimated convective heat transfer coefficient, respectively, the unit is $W/(m^2 \cdot K)$; T_{exp} and T_{est} are the experimental and estimated temperature data of a certain point for the fluid at a certain time step, respectively; the unit is °C; U is the total number of time nodes.

The estimated results for the four cases are shown in Table 1, Table 2 and Fig. 8. It can be seen that as the standard deviation σ becomes large, the relative error ε_h and the average absolute error $\bar{\varepsilon}_T$ both increase. However, the largest standard deviation and average absolute error are still within the acceptable range. In other words, the method proposed in the work is accurate and has reasonable noise immunity.

TABLE 1. Estimated values of the convective heat transfer coefficient.

σ	0.0	0.1	0.5	1.0
h_{est} (W/(m^2·K))	2001.53	2002.57	2004.16	2005.46
$\bar{\varepsilon}_h$ (%)	0.077	0.129	0.208	0.273

TABLE 2. The average absolute error ($\bar{e}_T$/°C) in the estimated temperature data for the fluid near the inner wall.

	C-60°	C-90°	C-120°	D-0°
σ = 0.0	0.0064	0.0060	0.016	0.16
σ = 0.1	0.086	0.069	0.094	0.089
σ = 0.5	0.40	0.42	0.45	0.46
σ = 1.0	0.84	0.68	0.89	0.78

Through the IHCP, the transient temperature distribution of the solid area of the pipe wall from 0 s to 80 s can be obtained. For example, as Fig. 9 shown, it is temperature distribution of the inner wall and the outer wall at 50 s. Because of the excellent thermal conductivity of metal pipes, the temperature

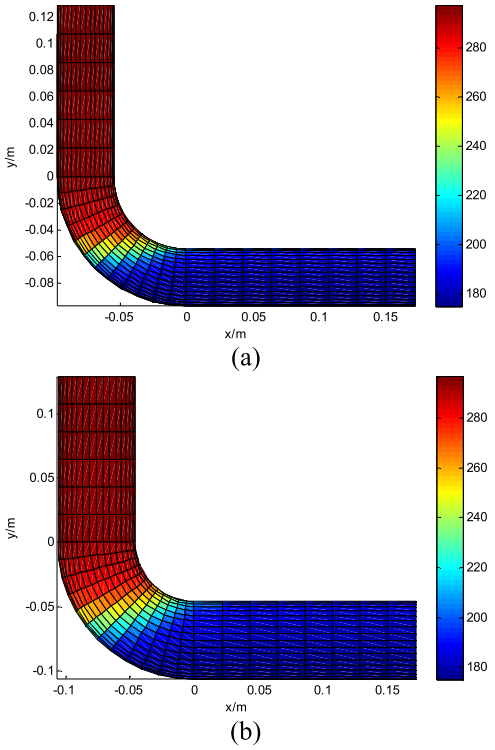

FIGURE 9. Temperature distribution of the inner wall and the outer wall at 50 s: (a) inner wall and (b) outer wall.

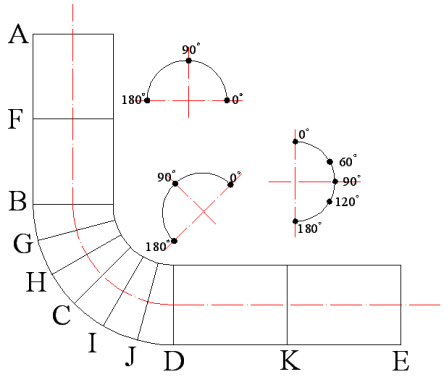

FIGURE 10. Measuring cross sections.

distribution of the inner wall and outer wall of the pipe is thermally stratified like that of the fluid. The time-dependent temperature data can provide significant information for the fatigue analysis of pipeline.

B. DISCUSSION ON THE NUMBER AND LOCATIONS OF MEASURING POINTS ON THE OUTER WALL

There are some errors in the actual measurement, therefore the standard deviation $\sigma = 0.5$ was chosen to discuss the number of measuring points on the outer wall. As shown in Fig. 10, measuring section F and K were arranged in the middle of the cross sections of A and B and section D and E, respectively. Seven measuring sections were uniformly

TABLE 3. Number of measuring points on cross sections.

Total number of measuring points	measuring sections A and F	measuring sections B, G, C, I, J and D	measuring sections K and E
76	4	9	7
74	3	9	7
62	3	7	7
58	3	7	5
46	3	5	5
40	2	5	3

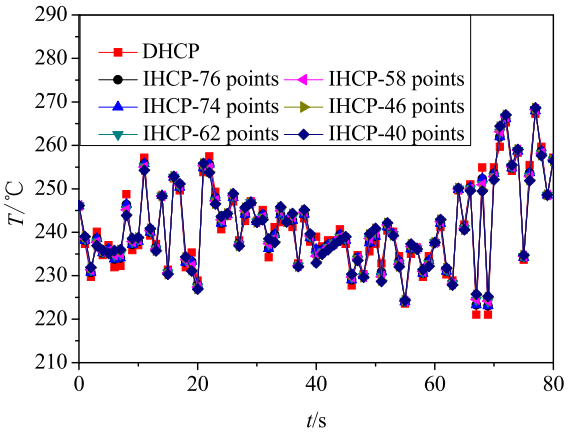

FIGURE 11. Comparison between experimental results and estimated results with different number of measuring points.

arranged between cross sections B and D, and keep cross sections B, C and D. The measuring points at each measuring section were arranged uniformly between 0° ∼180°. Six examples of different measuring points of outer walls were selected for discussion. The number of measuring points of each measuring section is shown in Table 3.

The measuring point cross section C - 90° where the fluid temperature fluctuates intensively was chosen to analyze the influence of number of measuring points on inversion accuracy. The estimated value of the fluid temperature based on different number of measuring points was shown in Fig. 11. It can be seen from the figure that the more the number of measuring points, the higher the degree of agreement with the experimental results., The estimated temperature fluctuations obtained from IHCP have good agreements with the temperature fluctuations of DHCP. In all cases, the minimum absolute error and maximum absolute error appear at the same time step, 60s and 40s respectively, and the error value increases with the reduction of the number of measuring points, i.e. 0.04°C ∼ 0.09°C and 2.89°C ∼ 6.02°C. As shown in Table 4, the average absolute error and average relative error of the estimated value of near-wall fluid temperature increase with the decrease of the number of measuring points. However, the calculation error of each adjacent two examples is basically the same. It can be seen from Table 3, there is the same number of measuring points in measuring sections B, G, C, I, J, D for the adjacent two examples. These indicate that the main measuring points affecting the calculation accuracy

TABLE 4. Average absolute error $\bar{e}$ and average relative error $\bar{\varepsilon}$ of the estimated fluid temperature at 90° on cross section C.

Total number of measuring points	$\overline{e}_T$ /°C	$\overline{\varepsilon}_T$ /%
76	1.023	0.426
74	1.024	0.426
62	1.519	0.632
58	1.570	0.653
46	2.026	0.843
40	2.127	0.885

TABLE 5. Estimated values of the heat convective coefficient with different measuring points.

Total number of measuring points	h_{est}/(W/(m^2 · K))	$\overline{\varepsilon}_h$ / %
76	2004.83	0.24
74	2005.16	0.26
62	2008.22	0.41
58	2008.75	0.43
46	2010.50	0.53
40	2011.12	0.56

are distributed on several measuring sections at the corner of the bend. The more the measuring points on these measuring sections, the higher the calculation accuracy will be; while the measuring points of other sections have less influence on the calculation accuracy. A similar conclusion can be drawn from Table 5 that the more the number of measuring points of several sections at the corner of the bend, the more accurate the estimated value of the convective heat transfer coefficient will be.

V. CONCLUSION

A transient three-dimensional IHCP with multi-variables has been developed using the CGM in order to estimate the convective heat transfer coefficient and the temperature fluctuations in a fluid near the inner wall based on the temperature data of the outer wall. And the sensitive analysis about the measuring errors and the number and locations of measuring points has been taken. The results show that:

(1) The transient temperature field of the whole solid area can be obtained through the IHCP.

(2) The convective heat transfer coefficient and the temperature fluctuations in the fluid near the inner wall can be estimated using the IHCP based on the CGM. The method avoids complex calculations of the convective heat transfer coefficient and direct measurement of the temperature of the fluid which could change the flow field.

(3) Comparisons of the estimated and the assumed experimental data for four representative cases have demonstrated the accuracy and noise immunity of the method.

(4) The more the number of measuring points on the outer wall, the higher the calculating accuracy will be, and the number of measuring points on several measuring sections at the corner of the elbow has a great influence on the calculating accuracy.

REFERENCES

[1] J. Rouse and C. Hyde, "A comparison of simple methods to incorporate material temperature dependency in the Green's function method for estimating transient thermal stresses in thick-walled power plant components," *Materials*, vol. 9, no. 1, p. 26, Jan. 2016.

[2] Y. Q. Li, W. Hu, Y. Sun, Z. Wang, and A. Mosleh, "A life prediction model of multilayered PTH based on fatigue mechanism," *Materials*, vol. 10, no. 4, p. 382, Apr. 2017.

[3] G. M. S. Ahmed and S. Algarni, "Design, development and fe thermal analysis of a radially grooved brake disc developed through direct metal laser sintering," *Materials*, vol. 11, no. 7, p. 1211, Jul. 2017.

[4] *Thermal Stresses in Piping Connected to Reactor Coolant Systems*, document US NRC 88-08, 1988.

[5] *Pressurizer Surge Line Thermal Stratification*, document US NRC 88-11, 1988.

[6] K. W. Bieniussa and H. Reck, "Piping specific analysis of stresses due to thermal stratification," *Nucl. Eng. Des.*, vol. 190, no. 1, pp. 239–249, Jun. 1999.

[7] I. Boros and A. Aszódi, "Analysis of thermal stratification in the primary circuit of a VVER-440 reactor with the CFX code," *Nucl. Eng. Des*, vol. 238, no. 3, pp. 453–459, Mar. 2008.

[8] T. Lu, H. T. Li, and X. G. Zhu, "Numerical simulation of thermal stratification in an elbow branch pipe of a tee junction with and without leakage," *Ann. Nucl. Energy*, vol. 60, pp. 432–438, Oct. 2013.

[9] T. Lu, X. G. Zhu, and H. T. Li, "Large-eddy simulation of thermal stratification in a straight branch of a tee junction with or without leakage," *Prog. Nucl. Energy*, vol. 64, pp. 41–46, Apr. 2013.

[10] J. I. Lee, L.-W. Hu, P. Saha, and M. S. Kazimi, "Numerical analysis of thermal striping induced high cycle thermal fatigue in a mixing tee," *Nucl. Eng. Des.*, vol. 239, no. 5, pp. 833–839, May 2009.

[11] T. Lu, W. W. Han, and H. Zhai, "Numerical simulation of temperature fluctuation reduction by a vortex breaker in an elbow pipe with thermal stratification," *Ann. Nucl. Energy*, vol. 75, pp. 462–467, Jan. 2015.

[12] Y. Ieda, I. Maekawa, T. Muramatsu, and S. Nakanishi, "Experimental and analytical studies of the thermal stratification phenomenon in the outlet plenum of fast breeder reactors," *Nucl. Eng. Des.*, vol. 120, nos. 2–3, pp. 403–414, 1990.

[13] A. Tokuhiro and N. Kimura, "An experimental investigation on thermal striping: Mixing phenomena of a vertical non-buoyant jet with two adjacent buoyant jets as measured by ultrasound Doppler velocimetry," *Nucl. Eng. Des.*, vol. 188, no. 1, pp. 49–73, Apr. 1999.

[14] N. Kimura, H. Ogawa, and H. Kamide, "Experimental study on fluid mixing phenomena in T-pipe junction with upstream elbow," *Nucl. Eng. Des.*, vol. 240, no. 10, pp. 3055–3066, Oct. 2010.

[15] T. J. Griesbach, P. C. Riccardella, and S. R. Gosselin, "Application of fatigue monitoring to the evaluation of pressurizer surge lines," *Nucl. Eng. Des.*, vol. 129, no. 2, pp. 163–176, Aug. 1991.

[16] C.-H. Huang and W. C. Chen, "A three-dimensional inverse forced convection problem in estimating surface heat flux by conjugate gradient method," *Int. J. Heat Mass Transf.*, vol. 43, no. 17, pp. 3171–3181, Sep. 2000.

[17] T. Lu, B. Liu, P. X. Jiang, Y. W. Zhang, and H. Li, "A two-dimensional inverse heat conduction problem in estimating the fluid temperature in a pipeline," *Appl. Therm. Eng.*, vol. 30, no. 13, pp. 1574–1579, Sep. 2010.

[18] T. Lu, B. Liu, and P. X. Jiang, "Inverse estimation of the inner wall temperature fluctuations in a pipe elbow," *Appl. Therm. Eng.*, vol. 31, nos. 11-12, pp. 1976–1982, Aug. 2011.

[19] T. Lu, W. W. Han, P. X. Jiang, Y. H. Zhu, J. Wu, and C. L. Liu, "A two-dimensional inverse heat conduction problem for simultaneous estimation of heat convection coefficient, fluid temperature and wall temperature on the inner wall of a pipeline," *Prog. Nucl. Energy*, vol. 81, pp. 161–168, May 2015.

[20] W. W. Han, H. B. Chen, and T. Lu, "Estimation of the time-dependent convective boundary condition in a horizontal pipe with thermal stratification based on inverse heat conduction problem," *Int. J. Heat Mass Transf.*, vol. 132, pp. 723–730, Apr. 2019.

[21] P. Duda, J. Taler, and E. Roos, "Inverse method for temperature and stress monitoring in complex-shaped bodies," *Nucl. Eng. Des*, vol. 227, no. 3, pp. 331–347, Feb. 2004.
[22] J. Taler, D. Taler, K. Kaczmarski, P. Dzierwa, M. Trojan, and T. Sobota, "Monitoring of thermal stresses in pressure components based on the wall temperature measurement," *Energy*, vol. 160, pp. 500–519, Oct. 2018.
[23] M. Jaremkiewicz, P. Dzierwa, D. Taler, and J. Taler, "Monitoring of transient thermal stresses in pressure components of steam boilers using an innovative technique for measuring the fluid temperature," *Energy*, vol. 175, pp. 139–150, May 2019.
[24] J. Taler, P. Dzierwa, M. Jaremkiewicz, D. Taler, K. Kaczmarski, M. Trojan, and T. Sobota, "Thermal stress monitoring in thick walled pressure components of steam boilers," *Energy*, vol. 175, pp. 645–666, May 2019.
[25] C.-R. Su and C.-K. Chen, "Geometry estimation of the furnace inner wall by an inverse approach," *Int. J. Heat Mass Transf.*, vol. 50, pp. 3767–3773, Sep. 2007.
[26] C.-H. Huang and M.-T. Chaing, "A transient three-dimensional inverse geometry problem in estimating the space and time-dependent irregular boundary shapes," *Int. J. Heat Mass Transf.*, vol. 51, pp. 5238–5246, Oct. 2008.
[27] C.-H. Huang and C.-Y. Liu, "A three-dimensional inverse geometry problem in estimating simultaneously two interfacial configurations in a composite domain," *Int. J. Heat Mass Transf.*, vol. 53, pp. 48–57, Jan. 2010.
[28] C.-H. Huang and J.-Y. Yan, "An inverse problem in simultaneously measuring temperature-dependent thermal conductivity and heat capacity," *Int. J. Heat Mass Transf.*, vol. 38, no. 18, pp. 3433–3441, Dec. 1995.
[29] S.-M. Lin, C.-K. Chen, and Y.-T. Yang, "A modified sequential approach for solving inverse heat conduction problems," *Int. J. Heat Mass Transf.*, vol. 47, pp. 2669–2680, Jun. 2004.
[30] B. Czél, K. A. Woodbury, and G. Gróf, "Simultaneous estimation of temperature-dependent volumetric heat capacity and thermal conductivity functions via neural networks," *Int. J. Heat Mass Transf.*, vol. 68, pp. 1–13, Jan. 2014.
[31] R. Yadav, C. Balaji, and S. P. Venkateshan, "Inverse estimation of number and location of discrete heaters in radiant furnaces using artificial neural networks and genetic algorithm," *J. Quant. Spectrosc. Radiat. Transf.*, vol. 226, pp. 127–137, Mar. 2019.
[32] A. Shidfar, G. R. Karamali, and J. Damirchi, "An inverse heat conduction problem with a nonlinear source term," *Nonlinear Anal. : Theor.*, vol. 65, no. 3, pp. 615–621, Aug. 2006.
[33] C.-S. Liu, "A two-stage LGSM to identify time-dependent heat source through an internal measurement of temperature," *Int. J. Heat Mass Transf.*, vol. 52, pp. 1635–1642, Mar. 2009.
[34] D. T. W. Lin, W. M. Yan, and H.-Y. Li, "Inverse problem of unsteady conjugated forced convection in parallel plate channels," *Int. J. Heat Mass Transf.*, vol. 51, pp. 993–1002, Mar. 2008.
[35] S. K. Kim, B. S. Jung, and W. I. Lee, "An inverse estimation of surface temperature using the maximum entropy method," *Int. Commun. Heat Mass*, vol. 34, no. 1, pp. 37–44, Jan. 2007.
[36] B. A. Anderson and R. P. Singh, "Effective heat transfer coefficient measurement during air impingement thawing using an inverse method," *Int. J. Refrig.*, vol. 29, no. 2, pp. 281–293, Mar. 2006.
[37] H. Wang, Q. Yang, X. Zhu, P. Zhou, and K. Yang, "Inverse estimation of heat flux using linear artificial neural networks," *int J. Therm. Sci.*, vol. 132, pp. 478–485, Oct. 2018.
[38] S. Deng and Y. Hwang, "Applying neural networks to the solution of forward and inverse heat conduction problems," *Int. J. Heat Mass Transf.*, vol. 49, nos. 25–26, pp. 4732–4750, Dec. 2006.
[39] J. Zueco and F. Alhama, "Simultaneous inverse determination of temperature-dependent thermophysical properties in fluids using the network simulation method," *Int. J. Heat Mass Transf.*, vol. 50, pp. 3234–3243, Jul. 2007.
[40] S. Huang, B. Tao, J. Li, and Z. Yin, "On-line heat flux estimation of a nonlinear heat conduction system with complex geometry using a sequential inverse method and artificial neural network," *Int. J. Heat Mass Transf.*, vol. 143, Nov. 2019, Art. no. 118491.
[41] M. Cui, X. Gao, and J. Zhang, "A new approach for the estimation of temperature-dependent thermal properties by solving transient inverse heat conduction problems," *Int. J. Therm. Sci.*, vol. 58, pp. 113–119, Aug. 2012.
[42] G. X. Yu, J. Sun, H. S. Wang, P. H. Wen, and J. W. Rose, "Meshless inverse method to determine temperature and heat flux at boundaries for 2D steady-state heat conduction problems," *Exp. Therm. Fluid Sci.*, vol. 52, pp. 156–163, Jan. 2014.
[43] M. Higuera, J. M. Perales, M. L. Rapún, and J. M. Vega, "Solving inverse geometry heat conduction problems by postprocessing steady thermograms," *Int. J. Heat Mass Transf.*, vol. 143, Nov. 2019, Art. no. 118490.
[44] T. Peng and Y. Liu, "3D crack-like damage imaging using a novel inverse heat conduction framework," *Int. J. Heat Mass Transf.*, vol. 102, pp. 426–434, Nov. 2016.
[45] G. Jinlong, L. Junyan, W. Fei, and W. Yang, "Inverse heat transfer approach for nondestructive estimation the size and depth of subsurface defects of CFRP composite using lock-in thermography," *Infr. Phys. Technol.*, vol. 71, pp. 439–447, Jul. 2015.
[46] O. M. Alifenov and I. Y. Gejadze, "Thermal loads identification technique for materials and structures in real time," *Acta Astronautica*, vol. 41, pp. 255–265, Nov. 1997.
[47] I. Cornejo, G. Cornejo, C. Ramírez, S. Almonacid, and R. Simpson, "Inverse method for the simultaneous estimation of the thermophysical properties of foods at freezing temperatures," *J. Food Eng.*, vol. 191, pp. 37–47, Dec. 2016.
[48] Y. Zhang, T. Lu, P. X. Jiang, Y. H. Zhu, J. Wu, and C. L. Liu, "Investigation on thermal stratification and turbulent penetration in a pressurizer surge line with an overall out-surge flow," *Ann. Nucl. Energy*, vol. 90, pp. 212–233, Apr. 2016.
[49] Y. Zhang and T. Lu, "Unsteady-state thermal stress and thermal deformation analysis for a pressurizer surge line subjected to thermal stratification based on a coupled CFD-FEM method," *Ann. Nucl. Energy*, vol. 108, pp. 253–267, Oct. 2017.

WENWEN HAN was born in Hebei, China, in 1985. She received the Ph.D. degree in power engineering and engineering thermophysics from the Beijing University of Chemical Technology, Beijing, China, in 2017.

She was a Postdoctoral Researcher in the postdoctoral research station of mechanical engineering with the Qingdao University of Science and Technology, from 2017 to 2019, where she is currently a Lecturer with the Academic Division of Engineering. Her research interests include inverse heat conduction problem, flow and heat transfer in chemical process, and materials science.

TAO LU was born in Jiangxi, China, in 1975. He received the Ph.D. degree in thermal energy and power engineering from the Dalian university of Technology, Dalian, China, in 2003..

He is currently a Professor with the College of Mechanical and Electrical Engineering, Beijing University of Chemical Technology. His research interests include transfer process prediction and enhancement, energy system integration optimization and energy conservation, micro-scale flow and heat transfer, thermal and force coupling analysis, and safety evaluation under complex conditions.

HONGBO CHEN was born in Shanxi, China, in 1985. He received the Ph.D. degree in machine design and theory from the Beijing University of Chemical Technology, Beijing, China, in 2017.

He is currently a Lecturer with the College of Electromechanical Engineering, Qingdao University of Science and Technology. His research interests include polymer processing, and chemical process heat and mass transfer.